Title
DAMAGE OF ZEOLITE Y IN THE TEM AND ITS EFFECTS ON TEM IMAGES

Authors
Csencsits, R.
Gronsky, R.

Publication Date
1987-09-01

LBL-22695 Rev. c.2
Preprint

Center for Advanced Materials

CAM

Submitted to Ultramicroscopy

Damage of Zeolite Y in the TEM and Its Effects on TEM Images

R. Csencsits and R. Gronsky

September 1987

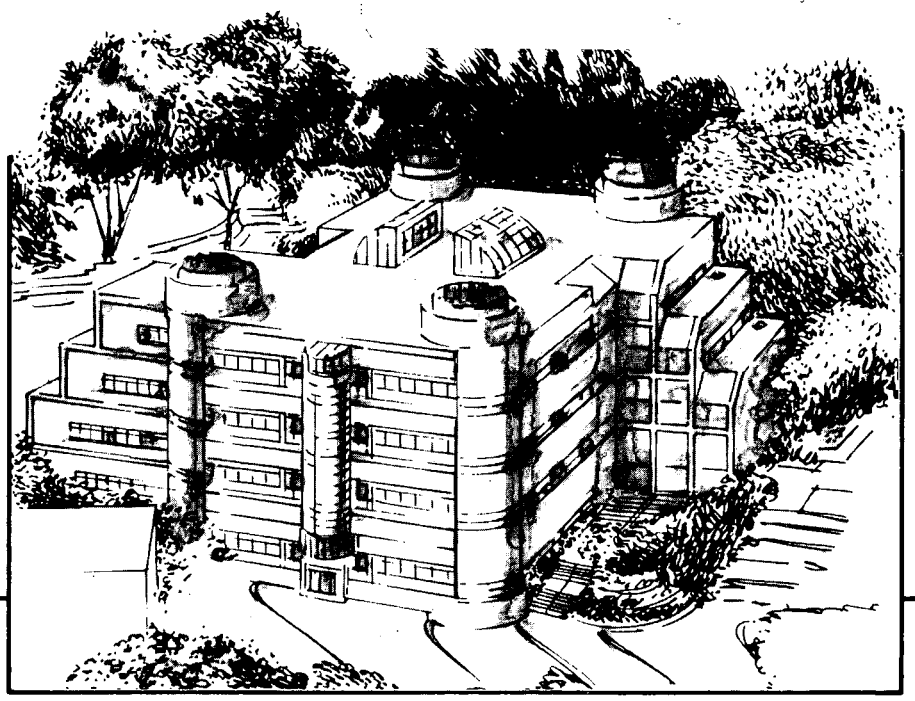

Materials and Chemical Sciences Division

Lawrence Berkeley Laboratory • University of California

ONE CYCLOTRON ROAD, BERKELEY, CA 94720 • (415) 486-4755

Prepared for the U.S. Department of Energy under Contract DE-AC03-76SF00098

DISCLAIMER

Damage of Zeolite Y in the TEM and its Effects on TEM Images

R. Csencsits and R. Gronsky

Center for Advanced Materials, and National Center for Electron Microscopy, Materials and Chemical Sciences Division, Lawrence Berkeley Laboratory, University of California, Berkeley, CA 94720

ABSTRACT

Electron diffraction has been used to study the vitrification of Y zeolite in the transmission electron microscope (TEM). Calculations and experimental evidence have confirmed that in the range 80-200kV, the damage of Y zeolites is radiolytic in the TEM. Incident beam electrons interact with specimen electrons which leads to a rearrangement of the structure. The proposed mechanism for this transformation involves enhancement of structural relaxation at Al sites due to the presence of a charge compensating cation.

Computer image simulation was used to assess the effects of damage on high resolution electron microscope (HREM) images of Y zeolites. Simulated images of perfect Y zeolite revealed that only for a specimen 10-20nm thick would the HREM image be a structure image at Scherzer defocus (-60nm); at thickness greater than 20nm the images contain non-structural detail due to second order interferences. At larger defocus values (-100nm), thicker crystals (60nm) "with 30-50% of their thickness amorphous" produce images which can be related to the structure because the presence of the amorphous material decreases the visibility of the non-structural detail.

1. INTRODUCTION

High resolution electron microscopy (HREM) is a valuable technique for studying catalyst systems because it gives direct information about the structure and the types and distribution of defects present in the structure. The vitrification of zeolites (and other silicates) during observation in the transmission electron microscope (TEM) has been well documented [1-6]. Observations show that the damage rate of zeolites depends on the Si/Al-ratio, on the size of the cations [2], and on the extent of hydration [1]. This work is a systematic investigation of the damage of zeolite Y in the TEM; the goals of this study are to propose a mechanism for damage of zeolite Y in the TEM and to assess the effects of damage on HREM images using computer simulation.

The types of damage possible in an electron microscope can be classified under two general headings: knock-on and radiolytic. "Knock-on" damage involves the interaction of the incident electron with the core of an atom in the specimen. An atom is "knocked" from its site, thereby changing the structure. Radiolytic damage involves the transfer of energy from the incident electron to the electrons in the specimen. The increase in energy of the specimen electrons results in bond breakage and consequently the possible alteration of the structure.

Knock-on Damage

The cross-section for direct interaction of the probing electron and the nuclear core of an atom in the specimen is called the knock-on cross-section. For relativistic electrons this cross-section is given by [7,8]

$$\sigma_n = \left\{ \frac{4\pi a_o^2 U_R^2}{(mc^2)^2} \right\} \left\{ \frac{Z^2(1-\beta^2)}{\beta^4} \right\} \left\{ \left(\Omega_r\right) + 2\pi\alpha\beta \left(\Omega_r\right)^{1/2} - (\beta^2+\pi\alpha\beta) \ln\left(\Omega_r\right) - 1 - 2\pi\alpha\beta \right\} \quad (1)$$

where:

$$\Omega_r = \frac{T_{max}}{T_{th}} \qquad T_{max} = \frac{2\,U_p\,(U_p + 2mc^2)}{Mc^2}$$

$$\beta = \left\{1 - \frac{1}{\left(\frac{U_p}{mc^2} + 1\right)^2}\right\}^{1/2}$$

U_p is the incident beam kinetic energy (keV), and mc^2 is the rest energy of the electron (511 keV). Mc^2 is the rest energy of the nucleus, α is Z/137, Z is the atomic number, U_R is the Rydberg constant (0.0136 keV), and a_o is the Bohr radius (0.053 nm). The maximum energy that an incident electron can transfer to a nucleus is T_{max}. The minimum energy necessary to move an atom off its lattice site into some metastable position is T_{th}, which depends directly on the atomic number.

All materials undergo direct displacement of atoms above their specific threshold energy. Above the threshold energy for the knock-on process, the cross-section for knock-on increases with increasing accelerating voltage. The potential damage due to electron- nuclear interaction becomes more severe as the incoming electron gets more and more energetic. At higher accelerating voltages the electron has enough energy to cause multiple damage events. The quantity, $N_d = \frac{T_{max}}{2\,T_{th}}$, takes into account the possible cascade of damage events. The knock-on damage cross-section includes the cross-section for displacement of an atom directly due to interaction with the electron wave and the probability of being displaced by another "knocked" atom, i.e., $\sigma_{kd}=\sigma_n \times N_d$. Its variation with accelerating voltage is shown for aluminum in zeolite Y in figure 1.

Radiolytic Damage

The relativistic cross-section for the interaction between the incident electron and the specimen electron is given by [9]

$$\sigma_e = \left(\frac{8\,\pi\,a_o^2\,U_R^2}{mc^2}\right)\left(\frac{Z}{T'_{th}\,\beta^2}\right) \qquad (2)$$

where: T'_{th} is the minimum energy that must be transferred to the electrons of the solid to produce atomic nuclear movement, Z is the number of electrons (usually the atomic number) belonging to the target atom, and a_o, U_R, mc^2 and β have the meanings described previously. The minimum energy T'_{th} is specific to each unique atomic site within the specimen and is related to the bond strength and the coordination number of the atom. The behavior of the cross-section for electronic interactions with accelerating voltage is determined by the parameter β^{-2}. This dependence is illustrated in figure 1 for the case of aluminum in zeolite Y. Note that the cross-section for ionization decreases significantly with increasing accelerating voltage up to 500 kV, then levels off to a constant value.

The experimental efficiency factor, ς, for radiolysis in silicates is 0.0001 [10]. That is, for every ionization event that occurs, the probability of structural rearrangement is 1 in 10,000. The cross-section for radiolytic damage is thus given by

$$\sigma_r = \sigma_e \times \varsigma. \qquad (3)$$

For zeolites the cross-sections for knock-on and radiolytic damage are of the same order of magnitude, and should both be considered when studying zeolites in the TEM, especially when accelerating voltages above 200 kV are used.

2. EXPERIMENTAL

In-situ damage

Samples of Y zeolite (with sodium cations) with Si/Al-ratios = 2.4, 18 and ∞ and REY (with rare earth cations) with Si/Al-ratio = 3.7 were investigated. Specimens for the TEM were prepared by embedding the zeolite powder in LR White acrylic resin and thin sectioning (50-80nm) with a diamond knife on a Dupont-Sorvall MT-6000 microtome [11]. Experiments were carried out in a JEOL 200CX HREM operating between 80 and 200 kV. Incident beam current was measured at the image plane with an electrometer and the current density at the specimen was determined using $\phi_{specimen}=(Mag)^2\phi_{image}$ (ϕ=current density).

The crystalline to amorphous transformation was monitored and recorded on photographic film as the loss of intensity in the Bragg reflections in the selected area diffraction (SAD) pattern with time. The SAD pattern was taken from a $5\mu m^2$ region in the center of a $20\mu m^2$ area of uniform current density. For each specimen at every accelerating voltage, the transformation was monitored several times to ensure the reproducibility of the data. The dose to vitrification was calculated by multiplying the current density by the total time of exposure.

Computer image simulation

The effects of radiolytic damage of Y zeolites on their high resolution electron microscope images was investigated using computer simulation. The goal was to determine how much of a specimen could be completely amorphous without serious detrimental effects to the image. The high resolution images were computed using the 81D version of the Simulated High Resolution Lattice Image (SHRLI) [12] programs running on the LBL VAX8600; the dynamical electron scattering calculation uses the multislice method [13].

Images were simulated for Y zeolite oriented with the electron beam down the [110] zone axis parallel to the channels. The atomic coordinates of Y zeolite were taken from work by Baur [14]. To reduce the computation time and since the difference in the scattering potential between Al and Si is negligible, the structural model used for Y zeolite was a framework consisting of silicon and oxygen atoms without cations or water molecules.

To simulate damage in the crystal an amorphous computational cell was created by randomization of the atoms in Y zeolite. Placement of all atoms was such that the interatomic distance between atoms was at least as large as their interatomic spacing in zeolite Y [15].

Dynamical electron scattering was used to simulate HREM images; the interactions of all diffracted beams enter into the calculations to produce the final electron wavefield at the bottom of the crystal. The number of diffracted beams used in the calculations must be

sufficiently large to account for this dynamical scattering. For these computations 2267 diffracted beams were propagated through the crystal. In order to do this, interactions were considered with 9089 phase-grating coefficients out to 25.85nm^{-1}. For accurate representation of the phase-grating by the 128 x 128 array [16], the slice thickness was 0.4998nm.

Images were computed for JEOL 200CX electron microscope (EM) parameters; viz, spherical aberration coefficient of 1.2mm, spread of focus halfwidth of 10nm, beam convergence of 0.5mrad, the objective aperture corresponded to 5.0nm^{-1} and admitted 350 diffracted beams. The maximum specimen thickness assumed was 60 nm; in general a good microtomed thin section is 45-60 nm thick.

3. RESULTS

In-situ damage

The dose to vitrification is plotted as a function of accelerating voltage for the three samples containing sodium cations in figure 2. For all samples, increasing the accelerating voltage improves their radiation tolerance. This indicates that the damage is radiolytic and that knock-on damage is not significant up to 200 kV accelerating voltage, as expected from figure 1. The difference between the dose to vitrification for the samples with Si/Al-ratios 2.4 and 18 is about 25%; for the sample with Si/Al =∞, the dose to vitrification is 3.5 and 5 times greater than that for the samples with Si/Al-ratios 18 and 2.4, respectively. Removal of all the aluminum from the framework produces a zeolite that is significantly more stable to electron irradiation.

Radiolytic degradation of SiO_2 in the TEM has been explained as the weakening of Si-O bonds by the incorporation of H_2O in the structure [9]. If this mechanism is responsible for degradation of zeolites then the increase in dose to vitrification with Si/Al-ratio should be explained by the different cross-sections for radiolytic damage for Si and Al in the zeolite structure. Using equation 2, the ratio of the radiolytic cross-sections for an all Si containing zeolite versus a zeolite with Si/Al=1 is $\frac{\sigma_{Si}}{\sigma_{AlSi}}$=0.90. This predicts that a zeolite structure containing as many aluminum atoms as silicon atoms should degrade with a dose to vitrification 90% that for degradation of the same zeolite containing only silicon atoms (all aluminum atoms replaced with silicon atoms). This does not explain the data shown in figure 2, where the sample containing 29% Al (Si/Al=2.4) has a dose to vitrification 20% that of the Si/Al=∞ sample.

The data in figure 2 indicate that the mechanism and therefore the efficiency of radiolytic damage in zeolites is different from that in quartz. The important difference is that with aluminum in the framework there are charge-compensating cations to balance the net negative charge of the framework. These cations facilitate a different mechanism for the degradation of aluminum-containing zeolites.

Figure 3a shows Al tetrahedrally coordinated to four oxygen atoms in the zeolite framework. When one Al-O bond is broken (fig. 3b), the Al can remain coordinated to only three oxygens and the cation can bond to the fourth oxygen. The Al is stable with three bonds and the cation is still near it for local charge neutrality, but now the structure is permanently changed.

This mechanism explains why zeolite structures are less electron beam sensitive when sodium ions are exchanged by larger cations [2], when the Si/Al-ratio is increased or when

dehydrated in vacuo [1]. When an Al-O bond is broken the larger cations, slowed by steric hindrance, do not move into the proper position to bond to the dangling oxygen; therefore the probability for reforming the original Al-O bond is high and the structure is preserved. The stability of a zeolite improves when the number of cations in the structure is reduced by either increasing the Si/Al-ratio or by using cations with greater ionic charge. As the Si/Al-ratio increases the number of possible degradation sites decreases and the zeolite is more stable to electron irradiation. Rare earth cations such as La^{3+} are strongly stabilizing due to their large size and charge, see figure 4. Adsorbed water in the zeolite structure can fill the role of a cation in the damage mechanism, by bonding to the dangling oxygen; thus, dehydrating the zeolite enhances its stability under the electron beam.

Computer image simulation

Figure 5 shows the projected potential map of the Y zeolite unit cell and the amorphous computational unit cell in the [110] projection. This is how the image would look using an ideal microscope with perfect resolution. In the projected potential map of Y zeolite the large ($\approx$0.74nm) and the small ($\approx$0.22nm) tunnels are seen clearly. The projected potential map of the amorphous cell does not show any periodicities or ordering; the structure is random.

Simulations of the HREM images of perfect Y zeolite (fig. 6, 100% perfect) at Scherzer defocus [17] (-60nm for the 200CX EM) reveal that only for a specimen up to 20nm thick would the image be close to a structure image [18]. In a structure image the details in the image correspond directly to features in the specimen; ie., dark areas represent a high potential, many atoms, whereas light areas correspond to few or zero atoms. A true structure image would look very much like the projected potential map viewed at the resolution of the microscope. The HREM images of the 100% perfect Y zeolite at thicknesses 10-20nm are not truly structure images because there are gray patches in the large tunnels in the images. This anomalous dark contrast is due to the contrast-transfer-function (CTF) [19] for the 200CX electron microscope. Figure 7 shows that the lowest frequency reflection from Y zeolite ($(1\bar{1}1)$ in the [110] orientation) is largely blocked by phase shifts in the objective lens of the microscope at -60nm defocus. Only approximately 21% of the amplitude of the {111} reflection is passed to contribute to the image, and it is this essentially "missing" frequency that produces the dark contrast at the tunnel positions [20].

For specimen thickness greater than 20nm at Scherzer defocus, the computed HREM images contain additional non-structural detail (fig. 6, 100% perfect). This non-structural detail results from second order interferences of the dynamically scattered electron waves [21]. Since most microtomed thin sections are 50-60nm thick, their electron microscope images should not be interpreted intuitively because their images will bear little or no direct resemblance to their projected potential.

Figures 8 and 9 (100% perfect) show the effects of larger values of defocus on the HREM images of Y zeolite. As the microscope is defocused beyond Scherzer defocus, the image detail can not be related to the structure except for the white areas corresponding to the large channels. The large channels are visible at larger defocus values because the CTF changes shape and allows more of the amplitude of the {111} reflection to contribute to the image.

The effects of vitrification on HREM images of Y zeolite are visible in figures 6, 8 and 9. The most obvious effect in the image for a specific thickness and defocus is a continuous loss of image contrast and sharpness with the loss of crystallinity. At Scherzer defocus (fig. 6) for a specimen with 60% perfect Y zeolite at a thickness 30nm or greater, the images have become

fuzzy shades of grey without any discernible detail. This loss of detail with increased damage occurs for all choices of specimen thickness and microscope defocus.

In some cases the loss of detail in the image due to vitrification can be an advantage, particularly when the details are not related to the structure. A thick crystal (60nm) at a large defocus (-100nm), with 70-50% of its thickness perfect (fig. 8), produces an image which appears to relate to the structure. These images are similar to the images of thin crystals of 100% perfect Y zeolite at optimum defocus (fig. 6, $\leq$20nm); both the large and small channels are visible. This is in contrast to the 60nm thick crystal with 70-50% perfect crystal at Scherzer defocus (-60nm) which shows non-structural detail, as does a 60nm-thick 100% perfect crystal. In thick crystals at large defocus values, the amorphous damage in the specimen reduces the visibility of the non-structural detail and produces HREM images that look like the structure.

4. CONCLUSIONS

Experiments have confirmed that the damage of Y zeolites in the TEM is radiolytic and knock-on damage is not significant in the range 80-200 kV. Experimental evidence supports a model for the degradation of zeolites in which structural relaxation is enhanced at Al sites due to the presence of a cation. When an Al-O bond is broken the aluminum atom remains bound to only three oxygen atoms and the cation moves into a position to bond to the dangling oxygen atom, thus preserving local charge neutrality; however, the structure is permanently changed.

Image simulation has shown that only under very specific conditions are HREM images of Y zeolite structure images. These specific conditions are not usually met under normal experimental conditions. The limitation of specimen thickness may perhaps be reduced by ion-thinning of the microtomed thin sections. A reduction in specimen thickness will decrease the non-structural details in the HREM images which are due to second order dynamical interactions of the electron waves.

The damage of Y zeolites generally results in a decrease in the contrast and the sharpness of the details in HREM images. If a crystal has less than 20% of its thickness amorphous, its HREM images are not significantly different from those of a perfect crystal and image interpretation is unchanged. As a specimen becomes "more and more damaged" there is a loss of detail in the image that can in some cases be serendipitous. At large defocus values (-100nm), thick crystals (60nm) with 30-50% of their thickness amorphous, produce HREM images which can be related to the structure because the presence of the amorphous material decreases the visibility of non-structural detail. This reduction in visibility of non-structural details can aid the interpretation of the images.

ACKNOWLEDGEMENTS

The authors would like to thank Dr. I.Y. Chan of Chevron Research Company for many helpful discussions and for providing some of the samples of zeolite Y. We would like to thank Dr. M.A. O'Keefe for his help in using the SHRLI programs. Dr. R. Kilaas is acknowledged for providing the curve in figure 7.

This work was carried out at the National Center for Electron Microscopy at Berkeley and has been funded by the Director, Office of Energy Research, Office of Basic Energy Sciences, Materials Science Division of the U. S. Department of Energy under Contract No. DE-AC03-76SF00098.

REFERENCES

[1] Bursill, L. A., Lodge, E. A., and Thomas, J. M., Nature **286** (1980) 111

[2] Bursill, L. A., Thomas, J. M., and Rao, K. J., Nature **289** (1981) 157

[3] Das, G., and Mitchell, T. E., Rad. Effects **23** (1974) 49

[4] Hobbs, L. W., and Pascucci, M. R., J. Physique **41**(C6) (1980) 237

[5] Pabst, A., Amer. Mineralogist **37** (1952) 137

[6] Pascucci, M. R., Hutchinson, J. L., and Hobbs, L. W., Rad. Effects **74** (1983) 219

[7] McKinley, W. A. and Feshbach, H., Phys. Rev. **74** (1948) 1759

[8] Seitz, F., and Koehler, J. S., Solid State Physics **2** (1956) 305

[9] Hobbs, L. W., 'Introduction to Analytical Electron Microscopy,' ed. J. J. Hren, J. I. Goldstein and D. C. Joy, Plenum Press, New York, 1979, 437

[10] Hobbs, L. W., EMSA Bulletin **15** (1985) 51

[11] Csencsits, R., Schooley, C., and Gronsky, R., J. Elect. Micros. Tech. **2** (1985) 643

[12] O'Keefe, M.A., and Buseck, P.R., Trans. Amer. Crystallogr. Asso., **15** (1979) 27.

[13] Goodman, P., and Moodie, A.F., Acta. Cryst. **A30** (1974) 280.

[14] Baur, W.H., Amer. Mineralogist **49** (1964) 698.

[15] Smith, J.V.,in ACS Monograph 171,"Zeolite Chemistry and Catalysis", (J. A. Rabo, ed.), ACS, Washington, D.C., 1976; p.17,49.

[16] Self, P.G., O'Keefe, M.A., Buseck, P.R., and Spargo, A.E.C., Ultramicroscopy **11** (1983) 35.

[17] Scherzer, O., J. Appl. Phys. **20** (1949) 20.

[18] Cowley, J.M., Ann. Rev. of Mat. Sci. **6** (1976) 53.

[19] Frank, J., Optik **38** (1973) 519.

[20] Chan, I.Y., Csencsits, R., O'Keefe, M.A., and Gronsky, R., J. Catal. **103** (1987) 466.

[21] O'Keefe, M.A., 37th Ann. Proc. Electron Microsco. Soc. Amer., ed. G.W. Bailey , Claitor's Publishing, Baton Rouge, LA, (1979) 556.

FIGURE CAPTIONS

1. Knock-on and radiolytic cross-sections versus accelerating voltage for Al in Y zeolite.

2. Dose to vitrification versus accelerating voltage for Y zeolites containing sodium cations, with Si/Al = 2.4, 18, ∞.

3a. Aluminum atom tetrahedrally coordinated to four oxygen atoms in the zeolite structure.
3b. Aluminum atom coordinated to three oxygen atoms in the damaged zeolite structure.

4. Dose to vitrification versus accelerating voltage for Y zeolites containing sodium cations, with Si/Al = 2.4, 18, ∞ and REY containing lanthanum and neodymium cations, with Si/Al = 3.7.

5. Projected potential map [110] for Y zeolite unit cell and the amorphous computational unit cell.

6. Computer simulated HREM images at Scherzer defocus (-60 nm) of 100%-50% perfect Y zeolite.

7. Damped contrast-transfer-function for the 200CX microscope at Scherzer (-60 nm) (a), formed by imposing the envelope function (b), on the undamped CTF (c). Y zeolite spacings are marked for the four lowest spatial frequencies.

8. Computer simulated HREM images of 100%-50% perfect Y zeolite at -100 nm defocus.

9. Computer simulated HREM images of 100%-50% perfect Y zeolite at -140 nm defocus.

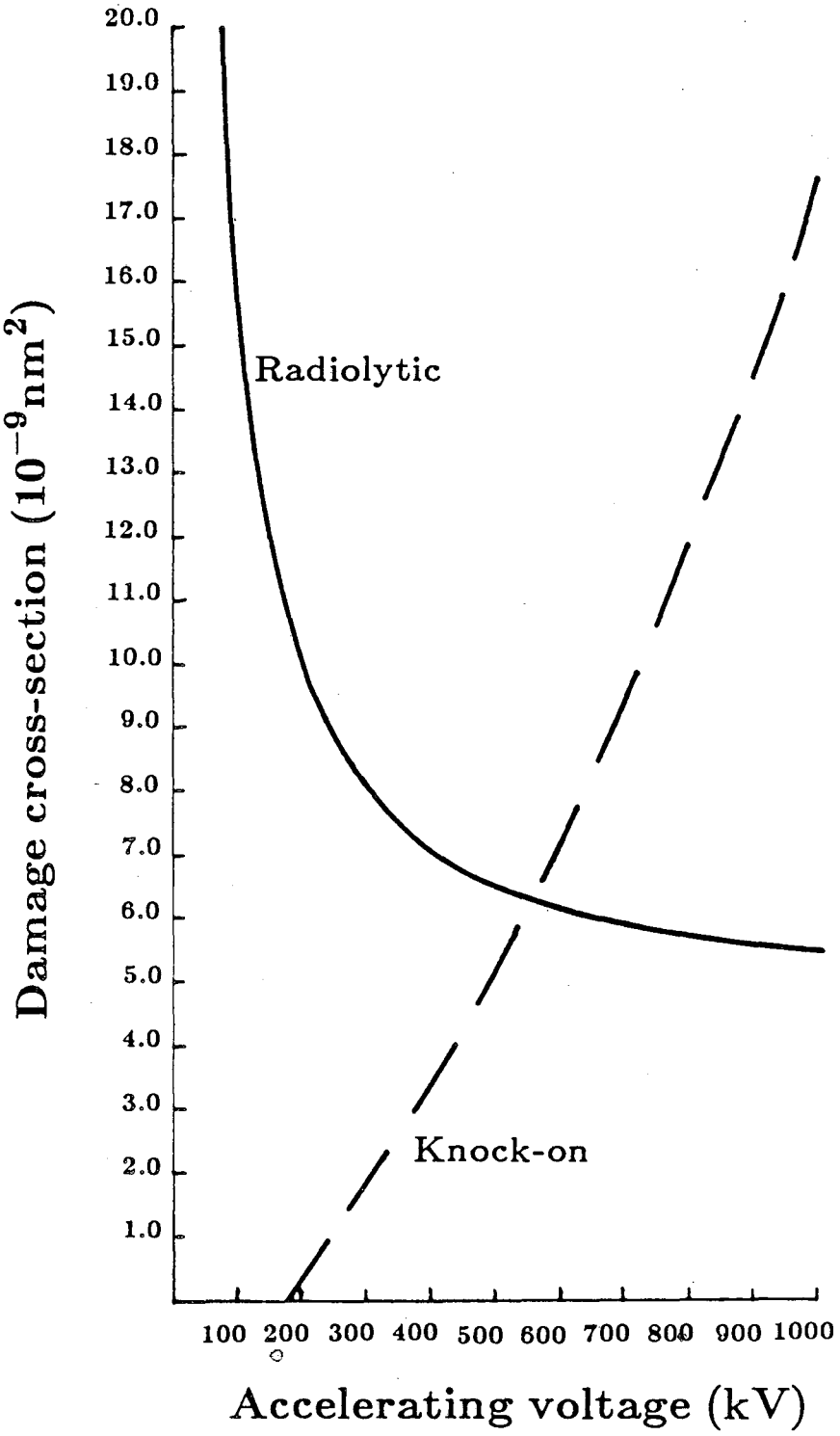

XBL 874-9272

Fig. 1

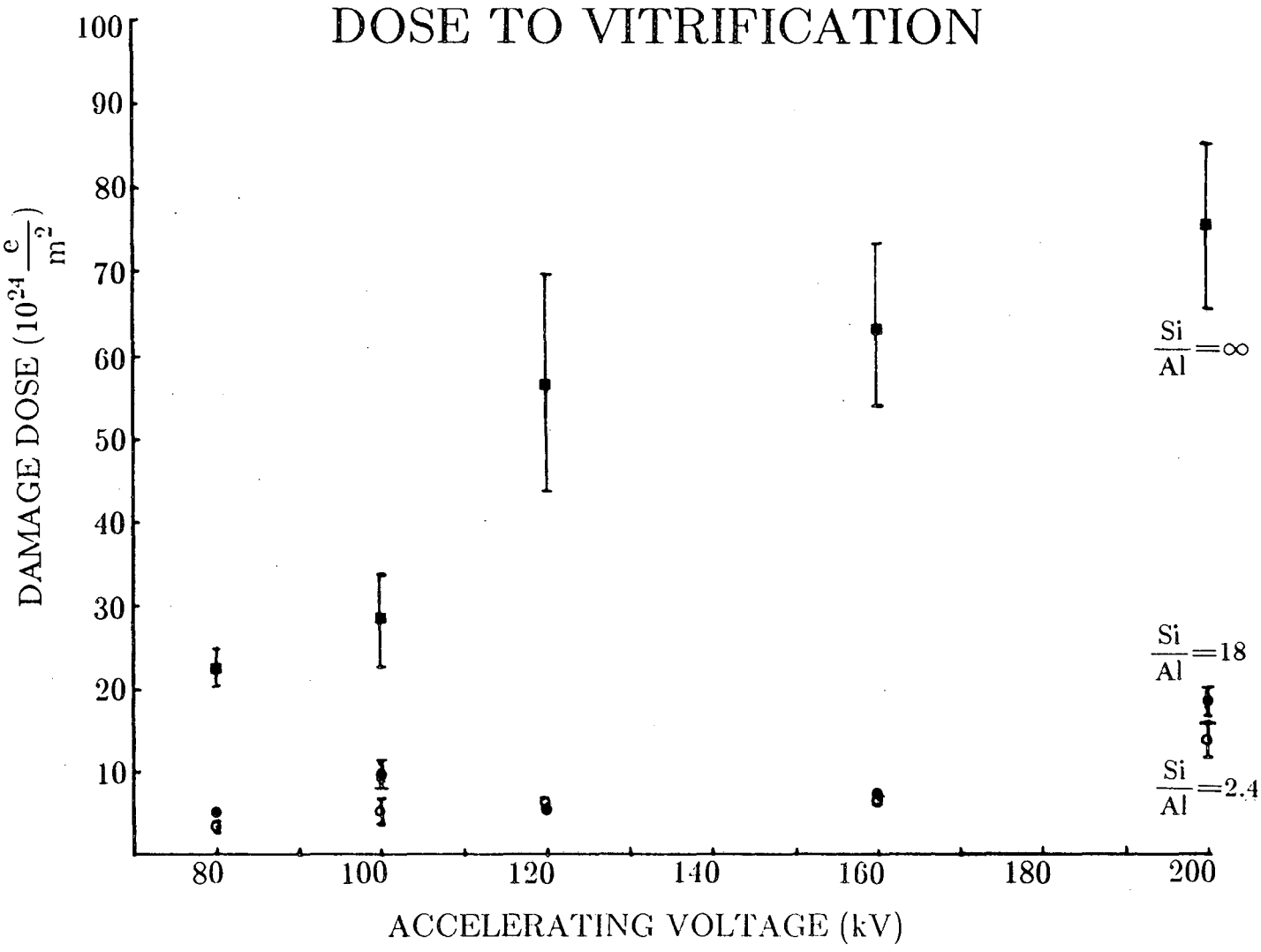

XBL 8511-4567

Fig. 2

Al in zeolite

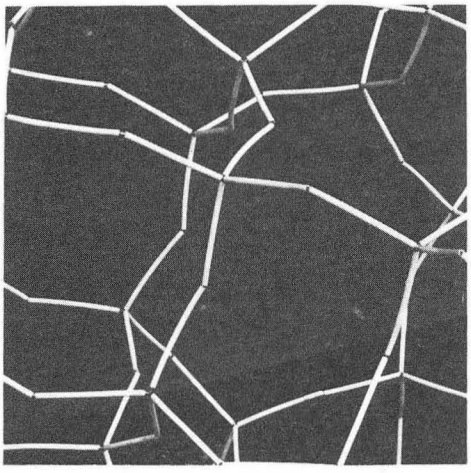

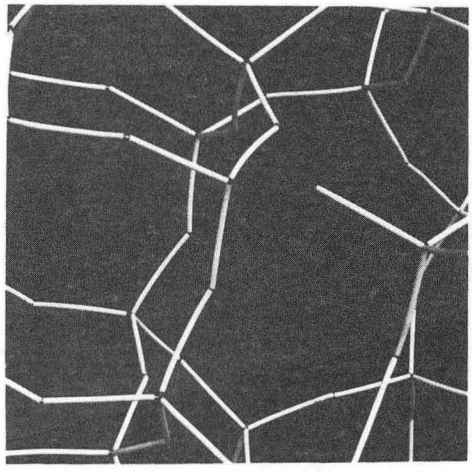

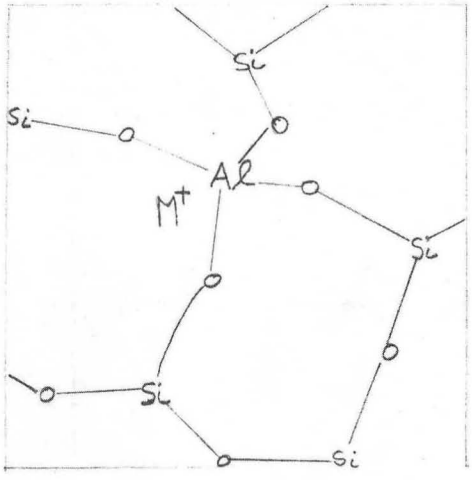

Al: 4 bonds

Cation: loosely bound

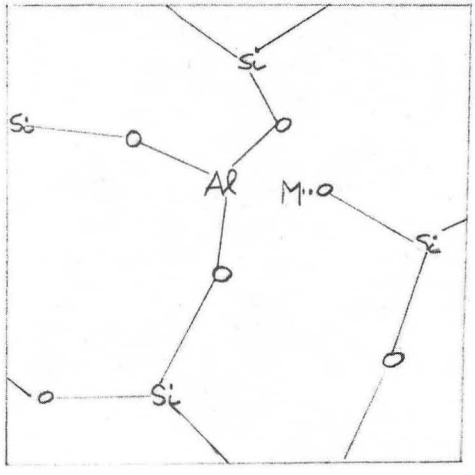

Al: 3 bonds

Cation: more tightly bound

XBB 867-5759

Fig. 3a

Fig. 3b

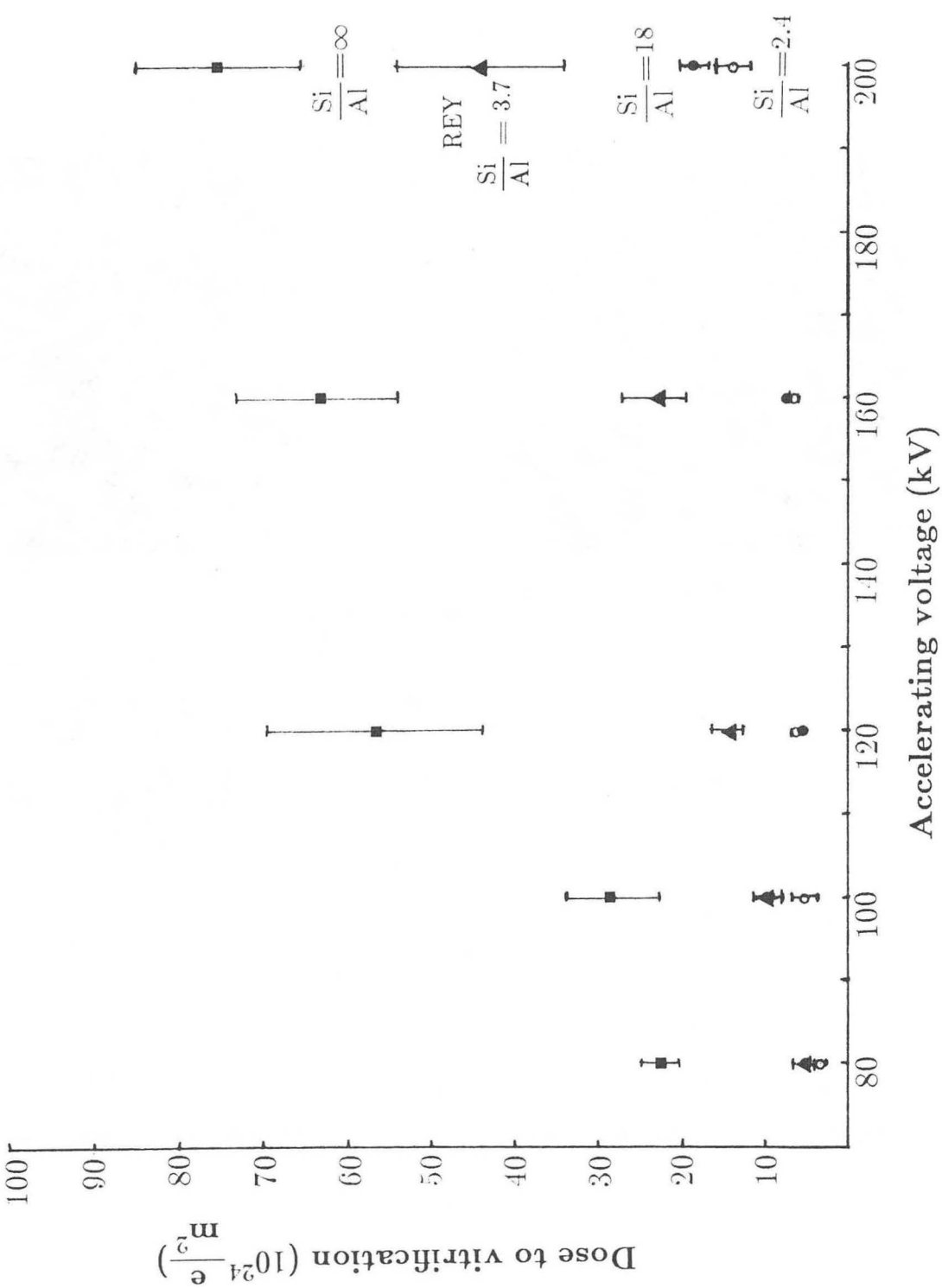

-- XBL 8612-4979 --

Fig. 4

Projected Potential [110]

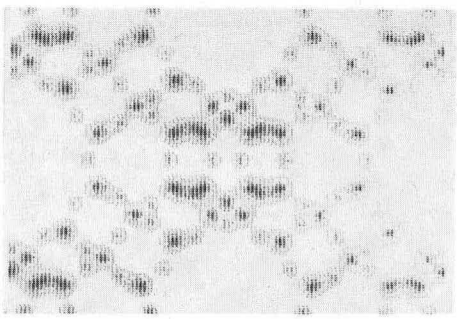

Y-Zeolite

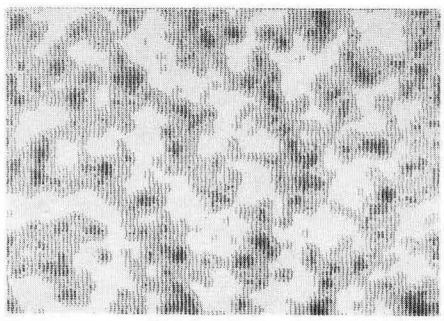

Amorphous

Fig. 5

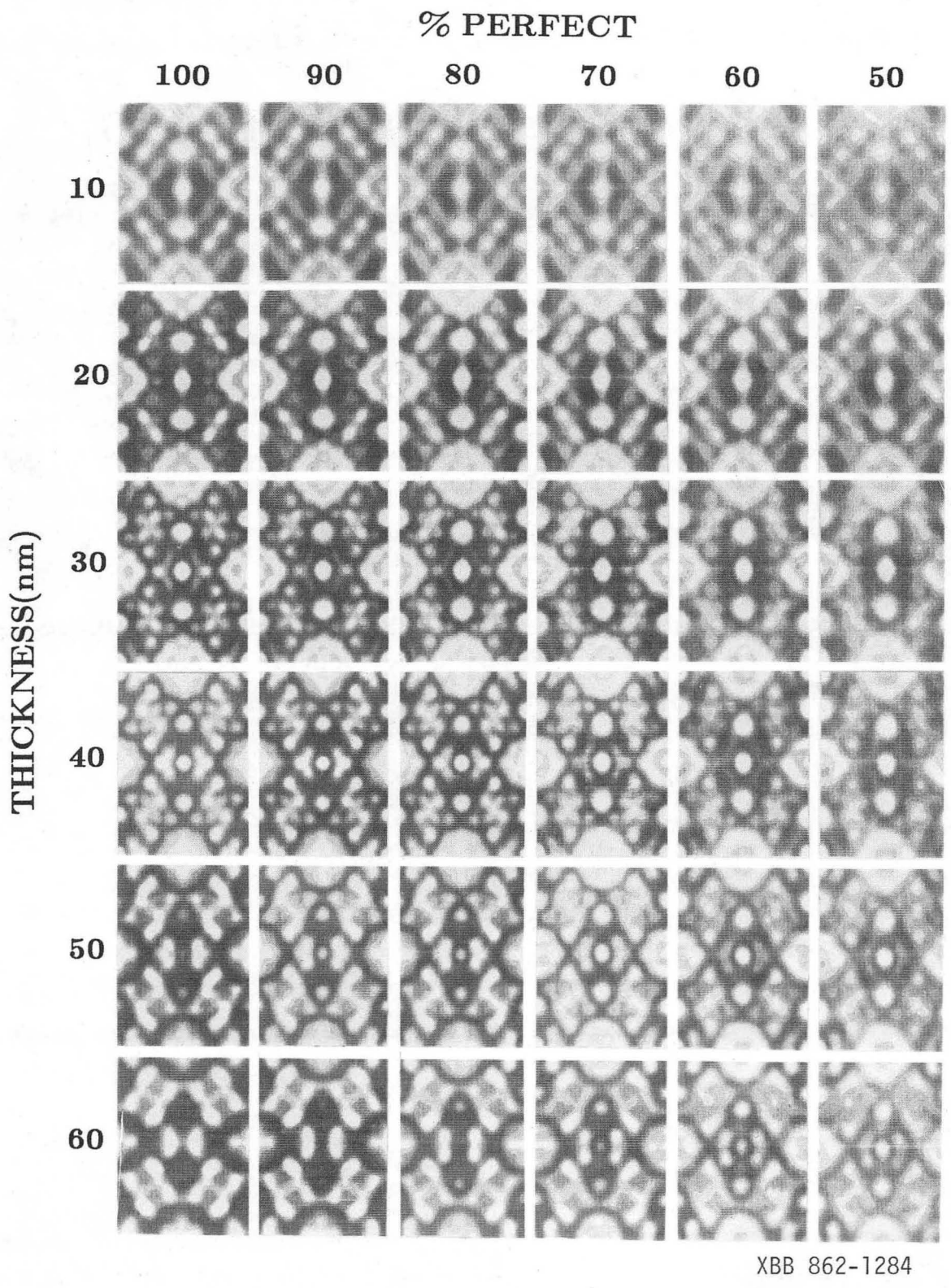
Δf=-60nm
% PERFECT
100
90
80
70
60
50
THICKNESS(nm)
10
20
30
40
50
60
XBB 862-1284

Fig. 6

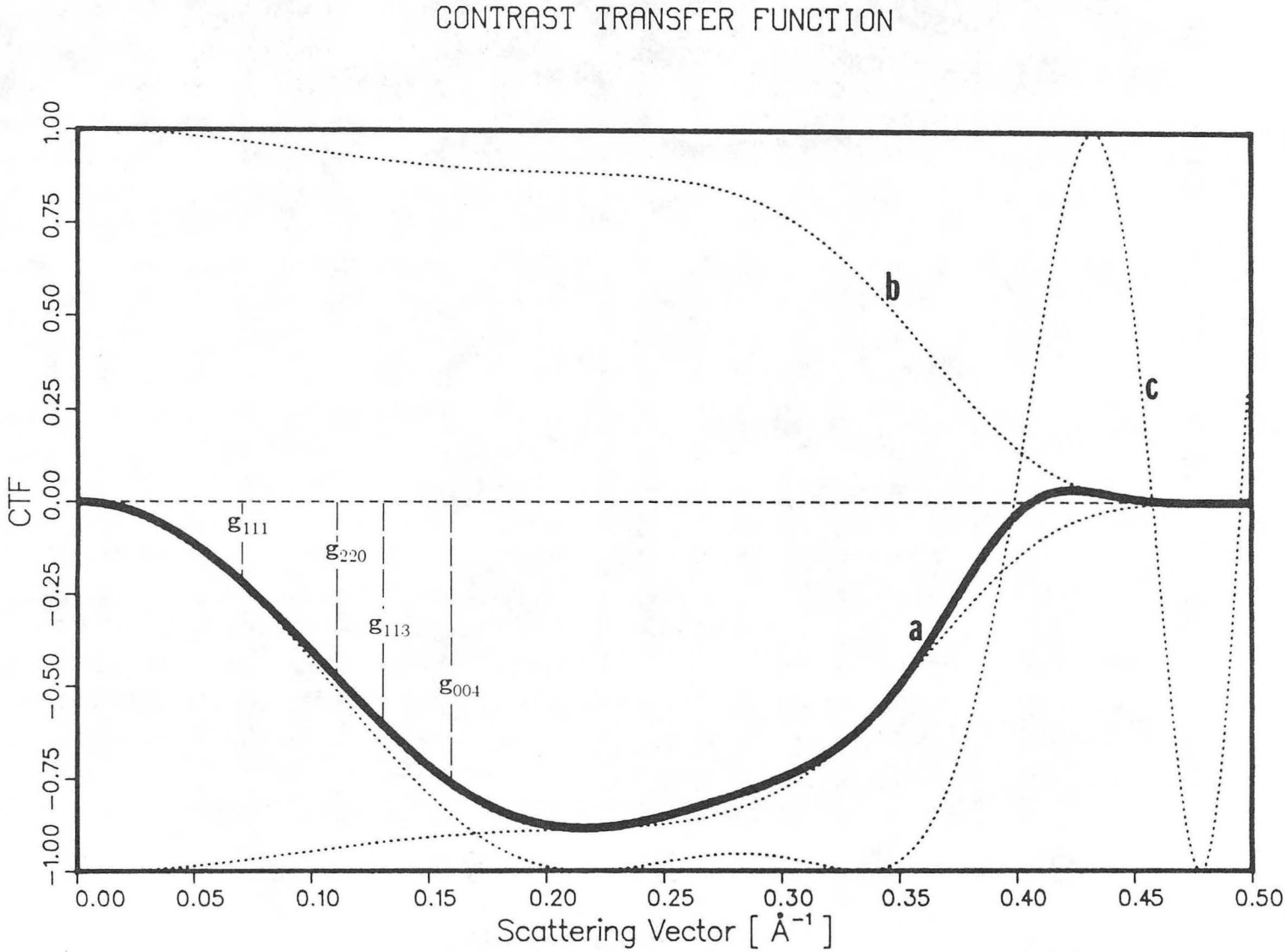

XBL 862-430

Fig. 7

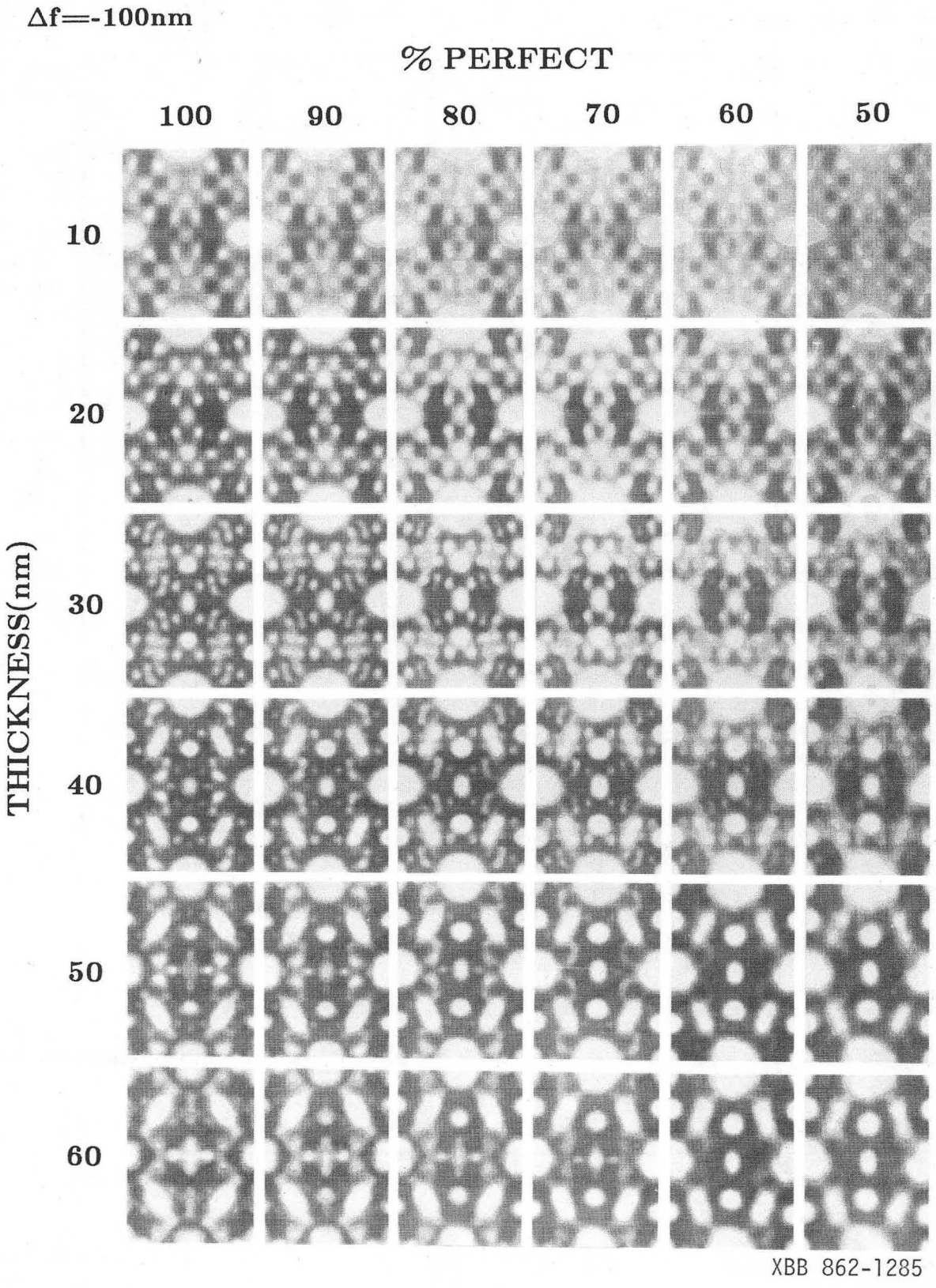
Δf=-100nm
% PERFECT
100
90
80
70
60
50
THICKNESS(nm)
10
20
30
40
50
60
XBB 862-1285

Fig. 8

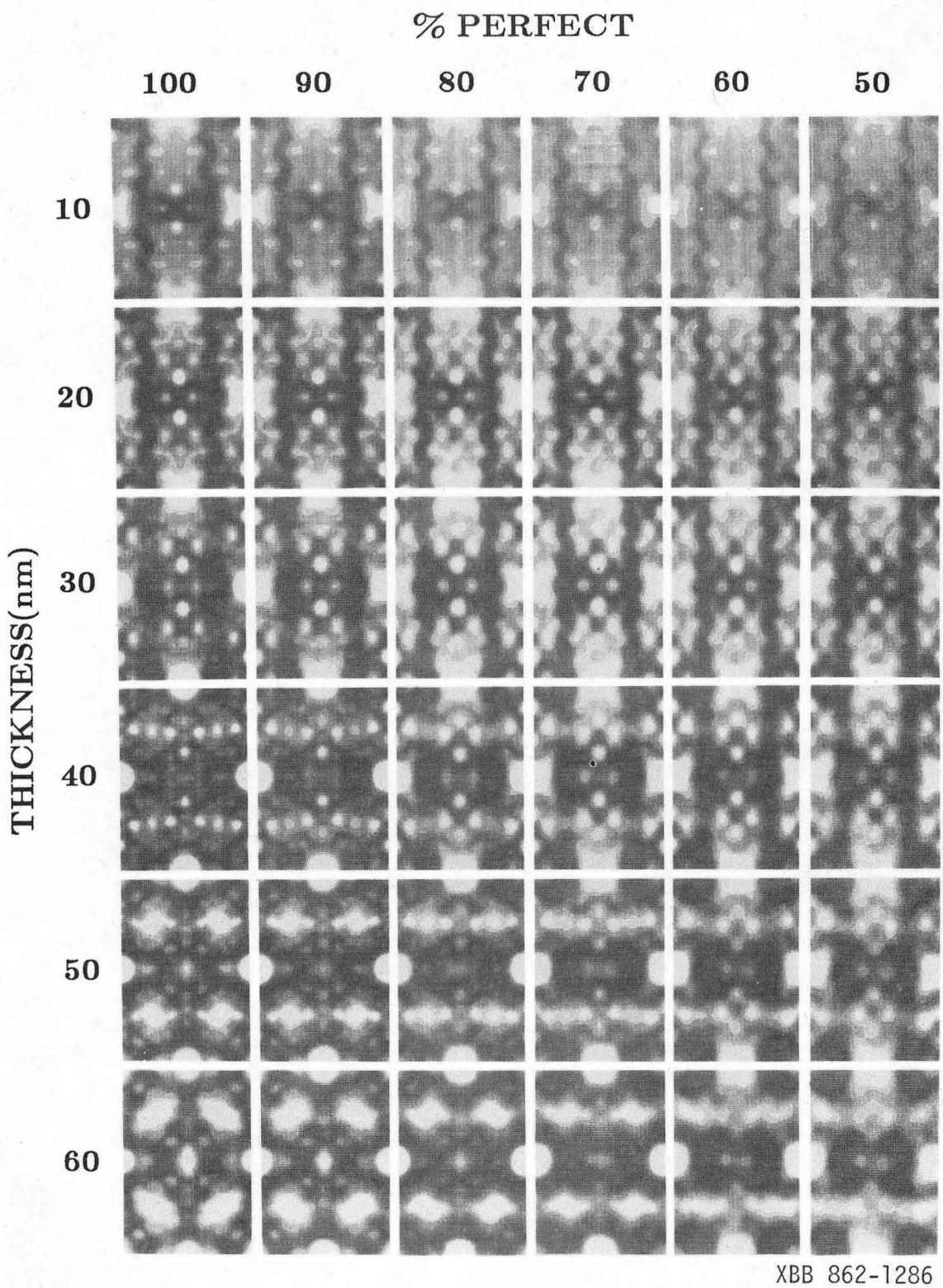
Δf=-140nm
% PERFECT
100
90
80
70
60
50
THICKNESS(nm)
10
20
30
40
50
60
XBB 862-1286

Fig. 9

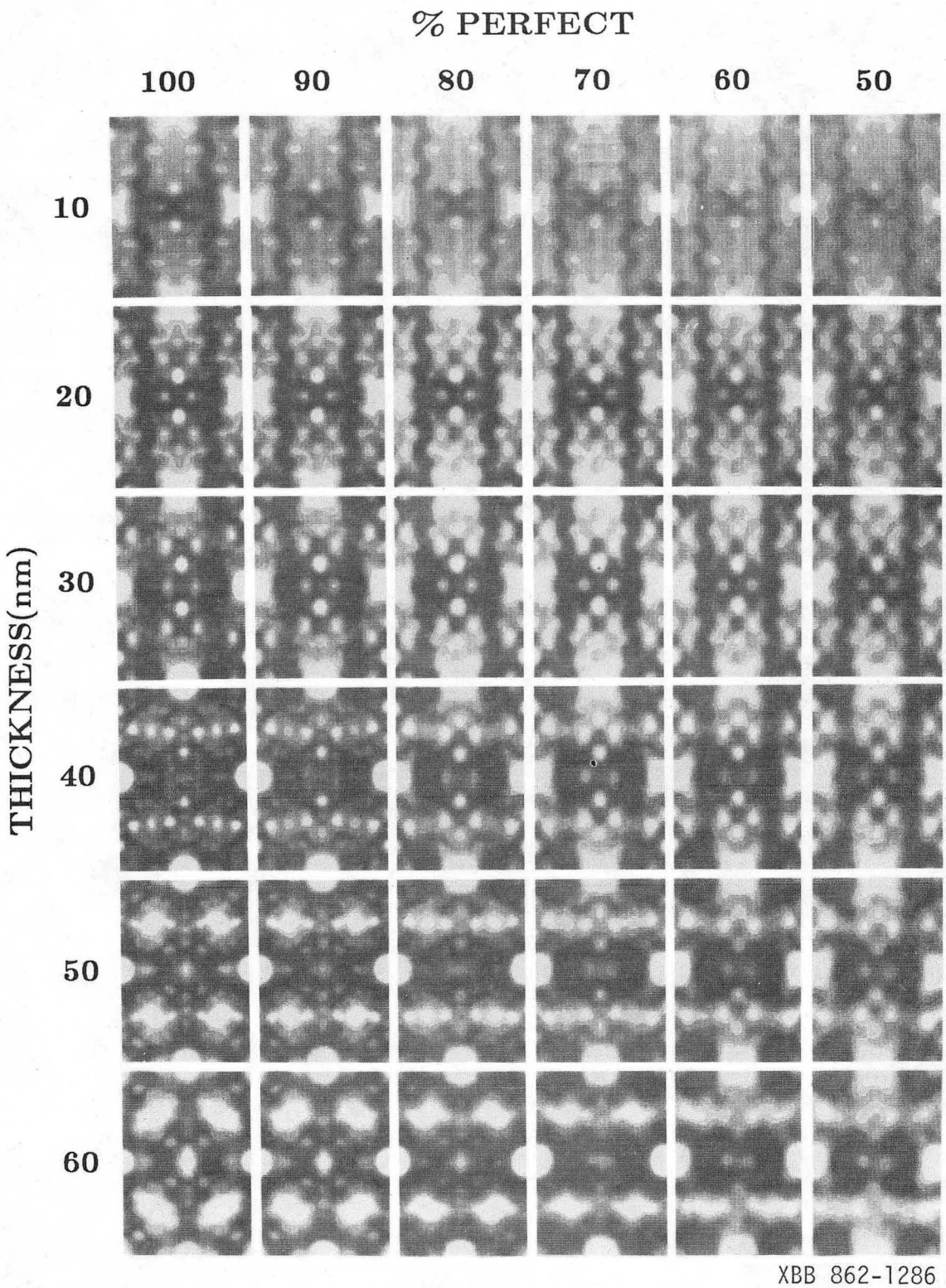
Δf=-140nm
% PERFECT
100
90
80
70
60
50
THICKNESS(nm)
10
20
30
40
50
60
XBB 862-1286

Fig. 9

LAWRENCE BERKELEY LABORATORY
TECHNICAL INFORMATION DEPARTMENT
UNIVERSITY OF CALIFORNIA
BERKELEY, CALIFORNIA 94720